Physics – Uspekhi **67** (8) 768 – 778 (2024)

REVIEWS OF TOPICAL PROBLEMS

PACS numbers: **07.87.+v**, **95.55.–n**, 98.80.Es

ON THE 90TH ANNIVERSARY OF THE P.N. LEBEDEV PHYSICAL INSTITUTE (LPI)

From the Spektr-R project to the Spektr-M project: milestones in space radio astronomy

S F Likhachev, T I Larchenkova

DOI: https://doi.org/10.3367/UFNe.2024.03.039662

Contents

Abstract. The main technical solutions implemented in the Spektr-R observatory (RadioAstron) and the scientific results obtained during its orbital operation from 2011 through 2019 are reviewed. General characteristics and research objectives of the Millimetron (Spectrum-M) space observatory, a development of the Spectrum-R project in the submillimeter wavelength range, are outlined. The launch of Millimetron is scheduled for the early 2030s. Research programs of both projects are led by the Lebedev Physical Institute of the Russian Academy of Sciences.

Keywords: radio astronomy, submillimeter astronomy, Spektr-R, RadioAstron, Spektr-M, Millimetron, radio interferometry, active galactic nuclei, jets, quasars, pulsars, masers, galaxies, supermassive black holes, wormholes, cosmic microwave radiation, interstellar medium, water in the Galaxy

1. Introduction

In the 1980s, four large-scale space projects of the Spektr series were proposed, which should span the main ranges of the electromagnetic spectrum. These projects are: Spektr-R (Radioastron) focused on studying space sources of radio emission in the wavelength range from 92 to 1.35 cm [1, 2]; the Spektr-RG Observatory (Spektr-Rentgen-Gamma) for observing cosmic objects in X-rays [3]; Spektr-UF (World Space Observatory–Ultraviolet) for studying sources of ultraviolet radiation [4]; and Spektr-M (Millimetron Space Observatory) for observing space objects in the millimeter and submillimeter wavelength ranges [5, 6, 76].

The creation of the Radioastron and Millimetron space observatories was proposed by academician Nikolai Semenovich Kardashev, a winner of USSR State Prizes. Under his guidance, the Radioastron project was implemented, and the development of the Millimetron Space Observatory began.

The Spektr-R radio telescope was launched into orbit on July 18, 2011 and operated in space until January 2019, exceeding more than twice the design life. The Spektr-RG X-ray space observatory, which was launched on July 13, 2019, is currently operating in orbit and transmitting unique data on cosmic X-ray sources [8, 9]. The launch of the Spektr-UF and Spektr-M space observatories is scheduled for the next decade.

We are proud to note that Spektr-R, developed at the Astro Space Center (ASC) of the Lebedev Physical Institute (LPI) in collaboration with Russian industry, was not only the first successful project in the Spektr series, but also the first major space project implemented in modern Russia. This project of the Federal Space Agency, the Russian Academy of Sciences, and international scientific community for the study of objects in the Universe in the radio range is unique in its scale and complexity. The Radioastron project allowed Russian scientists not only to return to the global VLBI (very-long baseline interferometry) community but also to obtain unique scientific results using this observatory. Joint observations of the Spektr-R space radio telescope with a mirror 10 m in diameter and the largest ground-based radio telescopes made it possible to materialize a ground-space radio interferometer with the largest base length, 350,000 km, which significantly enhanced the angular resolution of the observed objects compared to both ground-based radio interferometers and the previously implemented VSOP ground-space interferometer [10, 11].

S F Likhachev (*), **T I Larchenkova** (**)
Lebedev Physical Institute, Russian Academy of Sciences,
Leninskii prosp. 53, 119991 Moscow, Russian Federation
E-mail: (*) slikhach@asc.rssi.ru, (**) ltanya@asc.rssi.ru

Received 20 February 2024, revised 12 March 2024
Uspekhi Fizicheskikh Nauk **194** (8) 814 – 825 (2024)
Translated by M Zh Shmatikov

The Millimetron Space Observatory (Spektr-M), a logical extension of the Spektr-R project in the shorter wavelength range of the electromagnetic spectrum using technologies of the next level of complexity, is also being developed at the Astro Space Center LPI. The creation of this observatory will be the next step in the development of space instrumentation technologies and large space structures, which will ultimately enable the observatory's ambitious research program to be implemented.

Presented below is a brief overview of the technical solutions applied in and scientific results obtained by the Radioastron project and the research objectives of the Millimetron Space Observatory.

2. Radio telescopes and radio interferometers

Prior to discussing the Radioastron space project and the scientific results obtained through it, we make a brief introduction to radio astronomy. This field of science explores space objects that have emissions in the radio range of the electromagnetic spectrum, namely, in the wavelength band ranging from a few millimeters to tens of meters. Sources of radio emission are most space objects, such as galaxies, stars, planets, and clouds of interstellar gas. Released in the radio wave range is the energy of burst processes in active galactic nuclei and quasars and many processes occurring at shock wave fronts in the interstellar medium and during the interaction of turbulent gas jets. Rapidly rotating neutron stars with strong magnetic fields are observed as radio pulsars.

Cosmic radio emission was first discovered in 1931 by American radio engineer Karl Jansky while studying atmospheric radio interference. In 1937, Grote Reber designed the first radio telescope, which had a parabolic shape and an antenna about 9 m in diameter. This telescope was used to plot the first radio map of the sky at a wavelength of 1.5 m. The active development of radio astronomy began after World War II. Fully steerable parabolic radio telescopes with a diameter of 70–100 m were built in the USA, Germany, the UK, the USSR, and Australia.

The simplest radio telescope consists of an antenna, a receiver, and a recorder. The main characteristic of a radio telescope is its beam, which characterizes both sensitivity and angular resolution, determined by the width of the main lobe of the beam (see, for example, [12]). The width of the radio telescope beam is approximately equal to the ratio of the wavelength λ at which observations are made to the diameter of the telescope mirror D. Angular resolution characterizes the ability of a radio telescope to reconstruct an image of an observed source with a given level of detail, so the beam width determines the size of the smallest details of the source that are distinguishable individually. The λ/D ratio clearly shows that, to enhance resolution at a fixed wavelength, it is necessary to increase the diameter of the telescope.

To do so, it was proposed to 'synthesize' a large-diameter mirror from several individual antennas. The angular resolution of such a 'synthetic' instrument (radio interferometer) is determined not by the diameters of the individual antennas but by the distance between them, the so-called radio interferometer base D. If two antennas are located at a distance D from each other, the signal from a source arrives at one of the antennas slightly earlier than at the other. If the signals from the two antennas undergo interference, information about the source with an effective resolution can be extracted from the resulting signal using a special mathematical reduction procedure called aperture synthesis. It is of importance that receiving devices of each radio telescope and the communication lines that maintain coherence of the received signals when transmitted to the correlation processing center be identical. Interference can be realized by transmitting a signal through cables and waveguides to a common mixer. This is the operational procedure of multi-antenna coupled radio interferometers, the construction of which began in the 1960s.

Soviet researchers L Matveenko, N Kardashev, and G Sholomitsky [13] proposed to independently record observational data on each antenna and then process them together, which makes it possible to employ radio telescopes located at arbitrarily large distances from each other. This method is called very-long-baseline interferometry (VLBI). VLBI observations require using several radio telescopes equipped with the same type of receivers and recorders and a correlation processing center. In this case, what 'interferes' are the signals of the observed source previously digitized using exact time stamps and recorded onto media using appropriate software.

The base vector D has length $D = \Delta S/\cos\beta$, where β is the angle between the direction to the source and the base vector (Fig. 1). Since $\Delta S = v\tau$, where v is the speed of radio waves, the delay $\tau = (D/v)\cos\beta$. Thus, delay τ, which contains information about length D, is measured using a correlation method. Signals $S(t)$ recorded on telescope 1 and $S(t+\tau)$ recorded on telescope 2 are combined in a correlator, which outputs the correlation function $K(\tau) = \langle S(t)\, S(t+\tau)\rangle$ with a maximum at $\tau = 0$. The records are shifted until the maximum of the output signal is attained, and a delay τ equal to the shift value is determined.

Modern technical means enabled the creation of a VLBI system, which includes telescopes located on different continents and separated by several thousand kilometers. The VLBI method makes it possible to determine the length of the base vector with an error of 2–3 cm and the direction to the source with an accuracy of 0.001 arc seconds in both angular coordinates. The first transcontinental interferometers were implemented in 1968–1969 based on telescopes located in the USA and Sweden [14] and between deep space communication antennas in the USA and Australia [15, 16]. In 1969, US and Soviet radio astronomers carried out joint transcontinental interferometric observations using the 43-m telescope in Green Bank (USA) and the 22-m telescope in Simeiz (USSR) [17, 18].

Since dimensions of ground-based VLBI networks are limited by the size of Earth, to implement interferometer bases larger than Earth's diameter, it is necessary to launch a radio telescope into space [19]. In the late 1970s, KRT-10, the

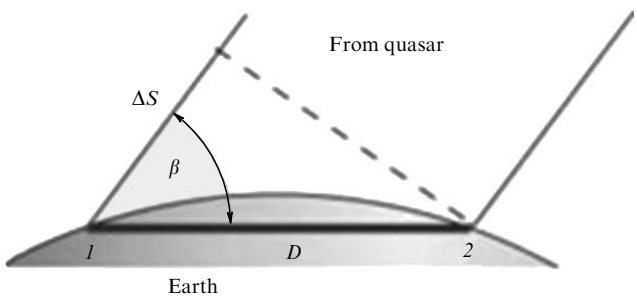

Figure 1. Illustration of radio interferometric method.

Figure 2. Liftoff of the launch vehicle with the Spektr-R space radio telescope and the Fregat upper stage on launch pad 45 of the Baikonur Cosmodrome on July 18, 2011. (From [2].)

first space radio telescope with a reflective unfurlable antenna, was created in the USSR. The telescope, 10 m in diameter and with a mesh reflective surface, was equipped with receivers for wavelengths of 12 and 72 cm. In the summer of 1979, this radio telescope was installed on the crewed orbital station Salyut-6, where astronomical observations were carried out [20, 21]. Operation of KRT-10 showed that space radio telescopes can be used to observe astronomical objects.

The first ground-space interferometers were implemented in the late 1980s in the USA [22, 23] and, in the late 1990s, in Japan (VSOP project [10, 11]). The Radioastron ground-based radio interferometer began operations in 2011 after the successful launch of the Zenit-3 F rocket with the Spektr-R spacecraft aboard on July 18, 2011 from launch pad 45 of the Baikonur Cosmodrome (Fig. 2).

3. Spektr-R project

The space radio telescope (SRT), which is part of the on-board scientific equipment of the Spektr-R spacecraft (SC) (Fig. 3), and the ground-based scientific complex were developed by the Astrospace Center of the Lebedev Physical Institute in close collaboration with Lavochkin research and production holding (AO NPO Lavochkina) and a number of Russian research and industrial organizations. Some devices of the onboard complex (rubidium frequency standard, 18-cm-range receiver, and high-frequency low-noise amplifier) were supplied by foreign organizations The Navigator spacecraft bus, which is part of the SC, and the SC ground control complex were developed by Lavochkin research and production holding with the participation of many organizations affiliated with the Russian Federal Agency for Space Research (Roskosmos).

3.1 Technical solutions in Spektr-R project

A detailed description of the SRT design, configuration, and parameters of the on-board scientific equipment and the ground control complex is presented in [2]. We list below the main components of the SRT and the ground segment. The Spektr-R observatory, which has a modular design, consists of the Navigator spacecraft bus, on which a reflector antenna 10 m in diameter and on-board scientific equipment are installed, including receiving equipment operating at wavelengths of 92, 18, 6.2, and 1.35 cm. The layout of the SRT and the hardware in the service module is shown in Fig. 4. To ensure high reliability of the service module (without manufacturing an experimental spacecraft for additional flight tests), components, systems, and assemblies that have been previously used on spacecraft were employed to the maximum extent possible. This approach significantly reduced the cost and time frame for developing the observatory by minimizing the volume of ground-based experimental testing, which was especially important given the limited funding for the project.

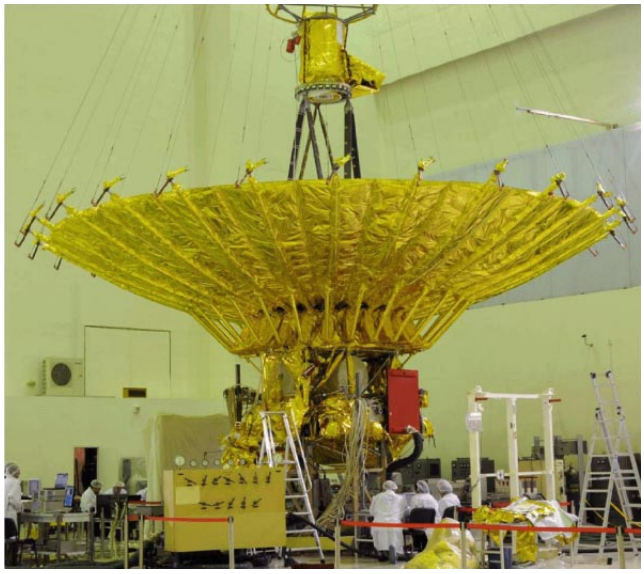

Figure 3. Spektr-R space radio telescope during final ground tests at Lavochkin research and production holding. (From [2].)

The SRT antenna was designed driven by the following requirements: a 10-meter antenna mirror should fit in the folded state in the rocket compartment under the head nose fairing with an internal diameter of 3.8 m, and the reflecting surface after unfolding should provide the required accuracy. Technical specifications require that the maximum permissible deviation of the radio telescope's mirror surface from the profile of an ideal paraboloid of rotation under all operating conditions should be ± 2 mm [2]. The reflective surface consisted of the central part of the mirror with a diameter of 3 m and 27 radial petal-shaped segments, synchronously unfolding in orbit. To obtain a high-precision reflective surface of the petals, the position of the petals was adjusted on the ground in a two-stage procedure.

The receiving complex consisted of on-board receivers that pick up signals in four wavelength ranges: P-KRT-92 receiver (P band with a center frequency of 324 MHz in the ± 7-MHz band), P-KRT-18 receiver (L band with a center frequency of 1664 MHz in the ± 30-MHz band), P-KRT-6M receiver (C band with a center frequency of 4832 MHz in the ± 55-MHz band), and P-KRT-135M receiver (K band with a center frequency of 22.232 GHz and seven more frequency sub-bands for multi-frequency synthesis in the frequency range of 18.372–25.120 GHz) [2]. Each receiver had two independent identical channels to which signals with left or right circular polarization were input from an antenna feed unit.

It is well known that of utmost importance in VLBI is frequency (phase) stability set primarily by the frequency

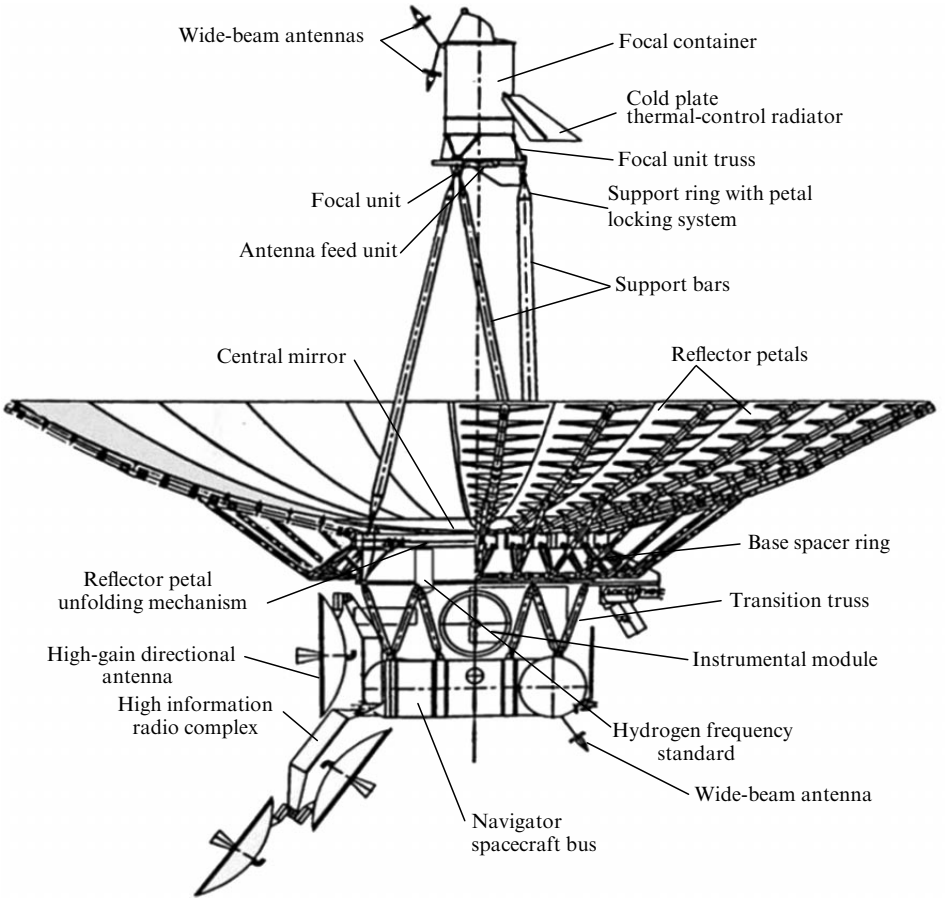

Figure 4. Layout of space radio telescope on Navigator spacecraft bus. (From [24].)

standard, the signal from which is used as the primary reference signal to carry out the necessary sequential frequency conversions. The SRT could operate with reference signals from three sources: an on-board hydrogen frequency standard of 5 MHz or 15 MHz, a 15-MHz signal of the phase-locking circuit of a high-information radio channel (HIRC) synchronized with a signal from a terrestrial hydrogen frequency standard installed at the tracking station, and an on-board rubidium frequency standard of 5 MHz. It should be noted that the SRT's onboard hydrogen frequency standard produced by the Vremya-Ch company was then the world's first on-board active hydrogen frequency standard launched to near-Earth orbit. HIRC is designed to transmit high-speed video information from a space radio telescope to a ground-based tracking station and to synchronize the on-board reference frequency with a signal from a ground-based hydrogen standard in one of two modes: 'COHERENT' or 'H-maser'.

An important feature of the Radioastron project was the choice of an orbit that strongly evolves under the influence of perturbations due to the Moon and the Sun. The orbital eccentricity varied from 0.96 to 0.59; the declination, from 10° to 85°; the perigee radius, from 7000 km to 81,500 km, and the apogee radius, from 280,000 to 353,000 km. To analyze data obtained using a ground-space interferometer, it is necessary to determine the position of its base with the highest possible accuracy, i.e., reconstruct the SC orbit with high accuracy. To determine the orbit, a motion model was used that takes into account the noncentrality of Earth's gravitational field, the attraction of the Moon and the Sun, the variable pressure of sunlight, perturbative accelerations due to reducing the torque of flywheels, and corrections to Earth's gravitational field due to its deformation under the influence of the gravity of the Moon and the Sun. The use of such a model made it possible to reconstruct the SC orbit for data processing in the correlator with a position accuracy of no worse than ±500 m and a velocity accuracy of no worse than ±2 cm s^{-1} in three coordinates.

On August 13, 2011, the first communication session was carried out with a ground-based tracking station deployed on the basis of the RT-22 radio telescope at the Pushchino Radio Astronomy Observatory (PRAO) of ASC LPI (Fig. 5). After

Figure 5. RT-22 radio telescope of PRAO ASC LPI in Pushchino.

that, measurements of the main parameters of the space radio telescope, the search for the lobes of the ground-space interferometer, and the implementation of the research program began. During the first three months after the launch, a program of flight tests of the on-board systems of the Navigator spacecraft bus was completed, confirming their compliance with technical requirements. For a number of parameters of the on-board systems, the actual characteristics obtained during flight tests significantly exceeded the requirements of the technical specifications, which made it possible to provide the best conditions for the implementation of the observatory's research program.

The first signal of the ground-space interferometer was received on November 15, 2011 based on observations of the quasar 0212+735 in an 18-cm range when the distance between the SC and Earth was about 100,000 km and the projection of the base between Radioastron and the 100-m radio telescope in Effelsberg (Germany) on the picture plane of the source was 8100 km [2]. It should be recalled that in interferometer mode the sensitivity of a two-telescope system is proportional to the square root of the product of the effective area of these telescopes; therefore, the sensitivity of a 10-m SRT and a 100-m ground-based radio telescope is equivalent to that of a system of two 30-m radio telescopes.

The first mapping was carried out using the results of observations at a wavelength of 6 cm by Radioastron–EVN (European VLBI Network) on March 14–15, 2012 of the quasar 0716 + 714, the distance to which is 1.6 Gpc; projections of bases ranged from1.5 to 7 Earth diameters [2]. In May 2012, interference responses from the quasar 2013 + 370 were recorded at the shortest wavelength of 1.35 cm and at a wavelength of 6 cm. Radioastron's early research program was implemented from February 2012 to June 2013 by international research teams formed within the project. From July 2013, a key research program based on open competitive applications commenced. The successful results of the early research program significantly raised the interest of the international scientific community in the Radioastron project, which manifested itself in a large number of applications for observations submitted by the world's largest radio astronomy observatories and leading astrophysicists. This also contributed to the inclusion in the project of a second ground-based tracking and scientific information collection station, the 43-meter radio telescope in Green Bank (USA).

One of the key segments of ground support for the Radioastron project is the Scientific Information Processing Center (SIPC) [26]. During the implementation of the project, about 60 ground-based radio telescopes located throughout the globe participated in observations as part of the interferometer. Each experiment involved up to 32 radio telescopes. The research data of approximately 428 PB from these radio telescopes was sent to ASC LPI for processing and storage. The results obtained from the Radioastron ground-space interferometer were processed and analyzed at ASC LPI. First, cross-correlation processing of data streams recorded by individual radio telescopes with a recording density of 128 or 256 Mbit s^{-1}, including that of SRT with 128 Mbit s^{-1}, was carried out. The correlation processing stage is the most important, resource-intensive, and computationally demanding operation of calculating visibility functions used in subsequent post-correlation analysis. The most important element of this process is the ASC LPI correlator [27], running on a computing cluster, the total performance of which was 1 Tflops in 2011 and more than 3 Tflops after 2018. The data streams at the correlator output are an integral measure of the quality of the entire Radioastron project and, essentially, they determine the successful outcome in solving scientific problems. The ASC LPI correlator operates according to the FX correlator scheme and provides necessary and well-known functions for regular daily correlation processing of data from multi-station VLBI networks with ground-based and ground-space bases. In total, data from over 4000 observational sessions of the Radioastron project were processed on the ASC LPI correlator.

For editing, calibration, post-correlation processing, and analysis of VLBI data at ASC LPI, the Astro Space Locator (ASL) software package was developed [28, 29], which provides a user-friendly graphical presentation of data and compatibility with all involved VLBI data processing systems. It was developed for Microsoft Windows in C++ using Microsoft Foundation Classes (MFC), but also runs on some Linux distributions (Ubuntu and Fedora) and on MacOS using Windows emulation software (WINE, Parallels, etc.). It is of importance to note that it is primarily due to the efficient operation of the correlator that the research program of the Radioastron project has been implemented, and unique scientific results have been obtained, which are discussed below.

3.2 Research program and results of Spektr-R project

The research program of the project was focused on studying the main types of compact sources with high brightness temperatures: active galactic nuclei (AGNs) and quasars, pulsars–highly magnetized rapidly rotating neutron stars, and galactic and extragalactic sources of maser radiation. Concurrently, an experiment was conducted to measure the gravitational redshift.

One of the main areas of the research program of the Radioastron ground-space radio interferometer was exploration of the nature of the radiation emitted by AGNs and quasars. Before the start of the Radioastron project, it was assumed that the radiation observed is the synchrotron emission of relativistic electrons from AGN jets and quasars. In such a model, the intrinsic brightness temperatures of sources cannot exceed $10^{11.5}$ K due to inverse Compton cooling [30, 31]. Note that the observed AGN emission may appear brighter due to Doppler gain related to the movement of the emitting plasma towards the observer (see, for example, [32]). However, modern VLBI observations of AGN jet kinematics indicate that the typical Doppler gain is 5–10 [33]. The ability of an interferometer to measure the brightness temperature of a source is determined by its sensitivity and the base projection. In the Radioastron project, the ground-space interferometer base length is up to 28 Earth diameters, which makes it possible to measure the brightness temperature of sources up to $10^{15} - 10^{16}$ K.

To measure the AGN brightness temperature, the 163 brightest sources were surveyed in three wavelength ranges: 1.3, 6, and 18 cm [34]. A large sample size is of importance both for modeling the effects of relativistic enhancement [35] and for investigating the typical value of the measured AGN brightness temperature. An analysis of observations showed that the measured brightness temperatures for the considered sample of sources exceed the Compton limit by a factor of 10 to 100 [34, 36]. Possible explanations for such extreme brightness temperatures

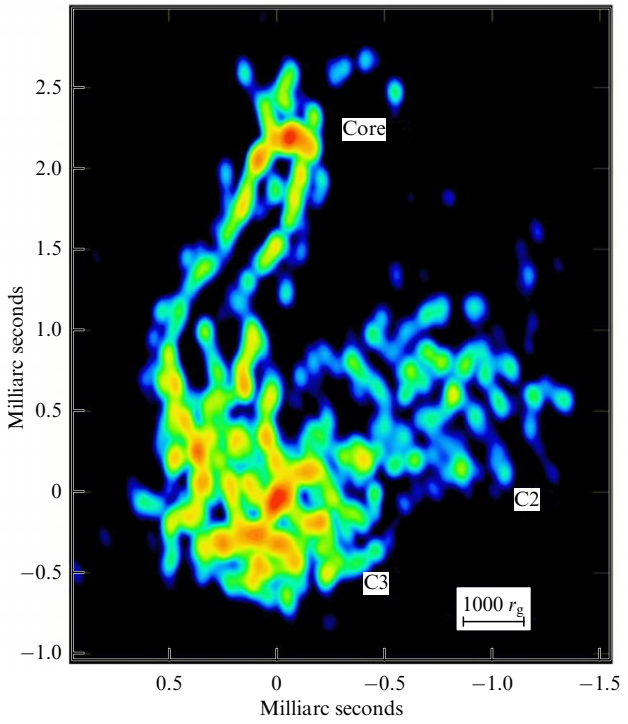

Figure 6. Radio image of central (parsec) region of 3S84 source obtained using Radioastron ground-space interferometer. Axes x and y show distance, in milliseconds of arc, from center of image. Marked on image are radio nucleus and bright emitting regions C2 and C3. (From [41].)

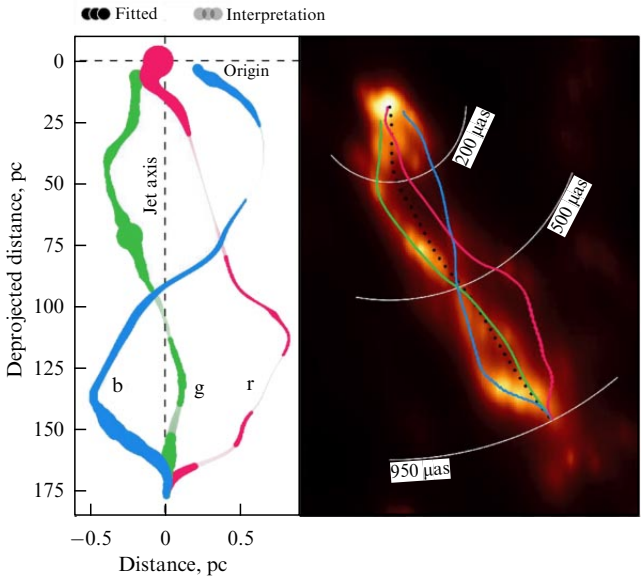

Figure 7. Filamentary structures in jet of quasar 3C 279 due to development of Kelvin–Helmholtz instability penetrated by a spiral magnetic field. Motion of radiating plasma along such filaments apparently causes the observed variability. Analysis of polarization structure and asymmetry of brightness distribution across jet made it possible to assess structure of the magnetic field, which is a spiral with a swirl angle of $\sim 45°$. (From [43].)

include the following: incorrect determination of the Doppler factor by VLBI methods, longer Compton loss times, magnetic reconnection of lines as a constant source of particle acceleration, and synchrotron radiation of protons [37, 38].

Another, no less important, question is: what is the structure of the magnetic field in the relativistic jets of quasars? According to modern concepts, the magnetic field is responsible for the formation and collimation of relativistic jets near the central supermassive black hole. Information about the polarization of the radio emission of such jets and the frequency spectrum enables exploration of their magnetic fields and the energy spectrum of the particles of their matter. To study the structure of the magnetic field, it is necessary to analyze spatially resolved linear polarization spectra, i.e., it is required to resolve the jets transversely at several observation frequencies. Such observations were implemented in the AGN survey and in the Radioastron polarization program, which included 20 experiments for mapping 10 sources with ultra-high angular resolution. As a result, it was found that, for many AGNs, the degree of linear polarization increases with increasing base of the ground-space interferometer, i.e., with angular resolution. This indicates the existence in the AGN of ultra-compact regions with a uniform magnetic field [39, 40]. In particular, based on the results of polarization mapping of the blazar BL Lacertae, the magnetic fields at the jet base were found to have a toroidal structure. For this source, the parameters of the visible core were measured, yielding a width at the jet base of approximately 70 μas or 0.3 pc [40].

The mapping enabled resolving many relativistic jets of quasars in a transverse direction, which made it possible to discover:

• brightening of radiation towards the edges of the jets as a result of stratification of the relativistic plasma flow (Fig. 6) [41, 45] and a subrelativistic shell around the jets, previously predicted based on the analysis of Faraday rotation [42];

• indications that the Blandford-Payne mechanism is preferable for the formation of a jet in the nucleus of radio galaxy 3S84, i.e., evidences the involvement of the accretion disk in this process [41];

• a hot plasma cocoon around a relativistic jet on parsec scales in the 3S84 source, providing supercollimation of a cylindrical jet [44];

• plasma instabilities in relativistic jets [43] (Fig. 7).

The next class of objects that Radioastron's research program explored are very compact sources of radio emission, pulsars. As a result of the propagation of radio emission from the pulsar to the observer, scattering occurs on inhomogeneities of the interstellar plasma, and a so-called scattering disk with angular dimensions of several milliseconds of arc in the meter radio wave range is formed. The project studied the parameters of the scattering disk of a sample of pulsars. Already the first observations of the brightest pulsar in the Northern hemisphere of the celestial sphere, B0329 + 54, showed that the scattering disc is not uniform but consists of multiple separated spots (peaks), which form the substructure of the scattering disk [48]. The discovery of this new phenomenon — the presence of a substructure of the scattering disk of pulsars — made it possible to reconstruct the parameters of effective scattering screens and estimate the distances to them and to detect indications of a layered structure of the interstellar plasma of our Galaxy [46, 52, 53]. It was shown that the effect of a scattering substructure should be taken into account in analyzing interferometric observation data with ultra-high angular resolution [47].

It should be noted that a similar effect has also been discovered for quasars [38]. A result of modeling the influence

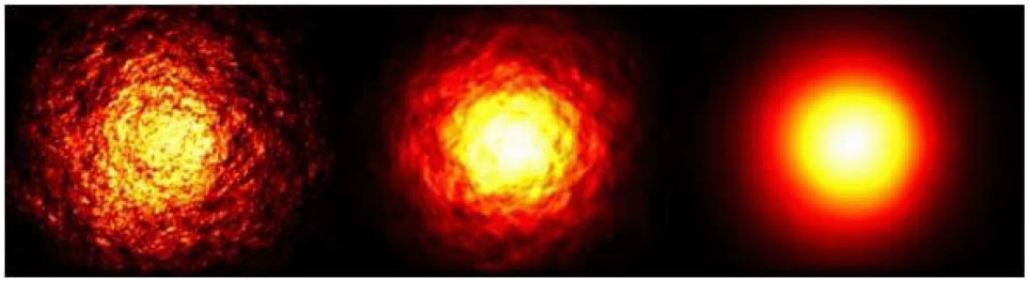

Figure 8. Result of modeling the influence of scattering substructure effect on source image for three wavelengths (from left to right): 18, 6.2, and 1.35 cm. (From [38].)

of the scattering substructure on the observed source image for three wavelengths, 18, 6.2, and 1.35 cm, is displayed in Fig. 8. In addition, an analysis of the structural and correlation functions of the observed scattered radio emission of pulsars led to the discovery of layers of interstellar plasma located close to the Solar System, which can result in rapid variability in the flux of compact extragalactic radio sources [49–51].

To study sources of maser radiation, the following programs were implemented: masers were surveyed in star-forming regions in our Galaxy to obtain estimates of the brightness temperature, flux density, and structure of the sources being studied; a number of the most promising sources were mapped to study in detail their fine spatial structure; and some extragalactic objects, so-called megamasers, were observed. Observations with a record spatial resolution of ~ 10 μs of arc enabled the discovery of compact features of high brightness in the water vapor disk of the megamaser in the galaxy NGC4258 and the presence of an extremely thin disk. This observational information is unique for understanding the conditions under which these unconventional sources of radiation are formed. In addition, evolving regions of water vapor were discovered inside the rotating central disk with a radius of about 0.126 pc [54]. The spectra obtained revealed the evolution of the velocities of the spectral components of water vapor with rapidly increasing and slowly decreasing activity in gas clusters of the central disk of the galaxy NGC4258. This type of shear instability of the radiation components involves a mechanism for the transfer of radial momentum and viscosity in the accumulated mass of the disk; therefore, the detected activity of the water vapor megamaser in NGC4258 may be associated with the magnetic-rotational instability that determines the rate of mass accretion in the central disk of the galaxy [54].

A bright burst of a water vapor maser in the source G25.25 + 1.05 was observed by the Radioastron interferometer when the SC distance from Earth was 9 Earth diameters. An ultra-compact maser-type object with angular dimensions not exceeding 25 μs of arc and a brightness temperature of 3×10^{16} K was discovered. Concurrent studies of the source G25.65 + 1.05 in a more quiescent state were carried out with the ground-based VLA array, and for the first time a map of maser spots in this source was obtained. It was concluded that the burst of a water vapor maser is explained by an increase in the size of the emitting region in the projection onto the line of sight as a result of the overlap of two molecular clouds in the picture plane [55].

At a distance of approximately 720 pc in the star formation region Cepheus A, sources of water vapor maser radiation comparable in size to the Sun were observed. To date, these objects are the smallest structures ever observed in our Galaxy's masers. It is assumed that they are associated with turbulent vortices in the gas flow from a massive star forming in the HW3dii region [56].

One of the impacts of the equivalence principle in the General Theory of Relativity (GTR) is the effect of gravitational time dilation, or gravitational redshift, which is actively measured. The essence of the gravitational redshift phenomenon is that, when an electromagnetic wave propagates in a gravitational field, its frequency f changes, and the relative change in frequency $\Delta f/f$ turns out to be directly proportional to the difference between gravitational potentials ΔU. If the equivalence principle is valid, the proportionality coefficient is equal to the inverse speed of light squared. As mentioned above, Radioastron concurrently conducted an experiment to measure the gravitational redshift. Thus, based on measurements conducted on just one SC orbit, the principle of equivalence of general relativity was verified with an accuracy of about 10^{-4}, which corresponds to that of the dedicated experiment Gravity Probe A [57–59].

4. Millimetron space observatory

As noted in the Introduction, the logical extension of the Spektr-R project to the shorter wavelength range of the electromagnetic spectrum is the Millimetron Space Observatory (Spektr-M), which is also being developed at the Astro Space Center LPI. Similar to the Spektr-R project, which provided not only unique scientific results but also a technological breakthrough in major scientific projects in today's Russia, Millimetron is a project of the highest level of technological complexity. The creation of such a high-tech instrument featuring high spatial resolution and sensitivity will allow researchers to solve a number of urgent problems in astrophysics and cosmology.

4.1 Technical characteristics of Millimetron observatory

The Millimetron Space Observatory (MSO) (Fig. 9) will operate in a wide range of wavelengths, from a few millimeters to 70 μm, in two modes: as a single space observatory with a 10-meter telescope and as part of a space–Earth interferometer [1, 5, 6]. The former mode will provide the best sensitivity for studying the faintest sources in the Universe. The latter mode will provide a high angular resolution of up to $10^{-8} - 10^{-9}$ seconds of arc, which will enable studying the structure of compact relativistic objects in the Universe. High sensitivity (0.1–1 μJy) is achieved via the large aperture of the primary mirror and deep cooling (to a temperature not exceeding 10 K) of the telescope mirror and on-board scientific equipment. High angular resolution is

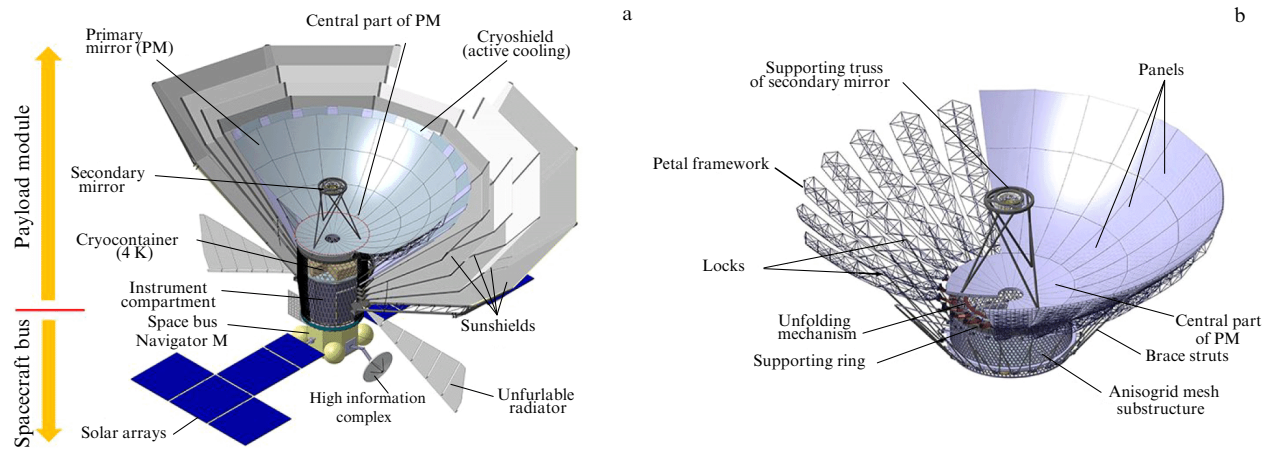

Figure 9. (a) Operational configuration of Millimetron Space Observatory; (b) design of primary mirror of observatory. (Figure from site www.millimetron.ru.)

ensured by, among other things, the orbital configuration. The observatory will orbit near the Lagrange point, L2, at a distance of 1.5 million km from Earth in the antisolar direction [60] (Fig. 10).

The telescope antenna, which is a Cassegrain two-mirror optical system, consists of a primary parabolic and secondary hyperbolic mirrors. Similar to the Radioastron project, the design of the primary mirror was developed based on the need to fit a 10-meter antenna mirror in the folded state into the rocket compartment under the nose fairing and ensure a high accuracy of the reflective surface after unfurling. The reflective surface is formed by the central part of the mirror, 3 m in diameter, and 24 radial petal-shaped segments [61], unfolding in orbit in space. The reflective surface of the panels and the main structure of the petals is made of high-modulus carbon fiber plastic [62], which features a low coefficient of thermal expansion. Each petal of the primary mirror consists of a frame and three independent reflective panels, which are mounted on the frame using linear actuators. To adjust the mirror panels, on-board surface control and adaptation systems are provided, which will correct deviations in the position of the panels associated with the unfolding process and distortions in the surface shape due to possible thermal deformations. It should be noted that the root-mean-square deviation of the surface of the entire antenna is 6 μm.

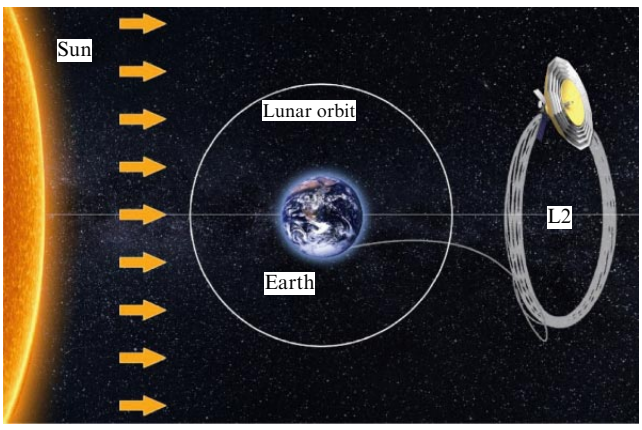

Figure 10. Image of the MSO halo orbit at the L2 point of Sun–Earth system with a period of 180 days. (Figure from site www.millimetron.ru.)

The concept of unfurling Millimetron observatory's primary mirror is based on experience gained from the Radioastron project. The petals are unfolded by rotation along one axis using a synchronous system, which reduces the complexity and enhances the accuracy of the antenna unfolding mechanism.

The MSO's scientific instrumentation will consist of individual receivers, each of which is optimized to solve specific research problems. Interferometric observations in the Earth-to-space mode will be carried out using VLBI receivers separated into frequency ranges corresponding to the ranges of the ALMA observatory and other ground stations. The frequency band spanned by VLBI receivers ranges from 33 to 373 GHz [63–65] with optional inclusion of an additional range of 490–650 GHz. To implement multi-frequency observations, a quasi-optical scheme is provided, which allows receiving a signal from the same direction in the sky.

It is noteworthy that the Millimetron project will carry out interferometric observations for the first time from the SC orbiting near the Lagrange point L2 at a distance of 1.5 million km from Earth. It was shown in [66] that, despite the limitations of such an orbit, it is possible to obtain a filling of the spatial frequency plane sufficient to reconstruct, with acceptable image quality, the shadows of central massive objects in the sources Sgr A* and M87* (Fig. 11).

For observations in single-antenna mode, a high-resolution spectrometer, a long-wavelength array spectrometer, and a short-wavelength array spectrometer will be employed. The high-resolution spectrometer, which operates in the frequency range from $\sim$ 500 GHz to $\sim$ 5 THz, includes seven separate heterodyne receivers operating in specified frequency ranges. The spectral resolution in all frequency ranges will be no less than 10^6, which will allow spectral observations to be carried out with very high resolution. Six of the seven receivers will be designed based on SIS and HEB mixers, which require deep cooling. The seventh receiver, duplicating the frequency range of the first one, 500–700 GHz, will be built using mixers based on Schottky barrier diodes, which will allow observations using this receiver to be conducted after the end of the active cooling period of the telescope.

The operating frequency range of the long-wave matrix spectrometer, from 100 GHz to 1 THz, is divided into four

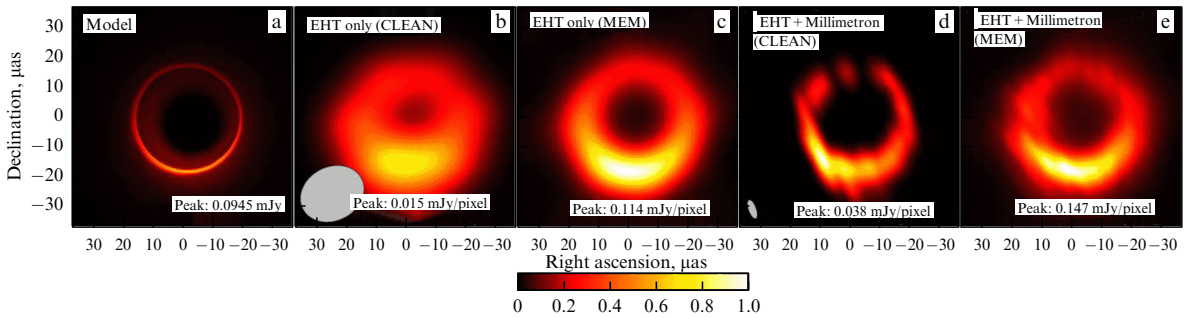

Figure 11. Model 2D images of shadow of a black hole in galaxy M87. (b, c) Results obtained by ground-based interferometer Event Horizon Telescope. (d, e) Results obtained using ground-space interferometer Millimetron–Event Horizon Telescope. (From [66].)

subranges. The device is primarily designed to obtain images and spectral and polarization information from low-intensity cosmic sources.

The operating frequency range of the short-wave array spectrometer, from 700 GHz to 6 THz, is also divided into four subranges. This highly sensitive instrument is designed to explore problems that require both photometric observations and broadband spectroscopy of medium spectral resolution, 10^3.

4.2 Main areas of Millimetron observatory's research program

The research program of the Millimetron space observatory is presented in detail in [76]. Here, we only outline the key ('breakthrough') scientific problems in three main areas of research: (1) the exploration of fundamental processes in the early Universe, (2) the study of the properties of space-time and matter in ultra-strong gravitational fields, and (3) the origin of life in the Universe. Solving the research problems in these areas will make it possible to answer a number of fundamental questions in physics, in particular: (1) what physical processes occurred in the early Universe in the pre-recombination era; what factors determined the parameters of the large-scale structure of the Universe; when and how did the first stars and galaxies emerge, and how do they correlate with those observed in the nearby Universe; (2) what is the structure of space-time in the vicinity of supermassive gravitating bodies; what is their nature; when and how did they appear; (3) how did life arise in the Universe; is it a unique or panspermic phenomenon in the Universe; what are its forms and observational manifestations.

The key research tasks of the three areas listed above are relevant for modern astrophysics and cosmology. In what regards studying basic processes in the early Universe, the key project is the detection of y- and μ-distortions in the frequency spectrum of the cosmic microwave background radiation [67–70], i.e., detection of deviations of this spectrum from the equilibrium spectrum of a black body. It is very challenging to extract information about the initial density fluctuations on small scales both from the analysis of the large-scale structure of the Universe due to the strong nonlinearity of the process by which it was formed on these scales and from the analysis of the angular anisotropy of the temperature distribution of the cosmic microwave background radiation due to the presence of dissipative processes in the baryon mass component (Silk damping [71]). Moreover, if in the pre-recombination era processes occurred in the Universe, which involved energy release, a trace of them remains in the frequency spectrum of the cosmic microwave background radiation, which is transformed from the Planck spectrum into the Bose–Einstein spectrum with a nonzero chemical potential μ. Measurements of the chemical potential of the Universe, which will make it possible to obtain restrictions on the spectrum of initial perturbations and information about the possible existence of primordial black holes, particles with a lifetime of $10^9 - 10^{10}$ s, and the dissipation of acoustic waves, are key research tasks of the observatory.

State-of-the-art methods of observational radio astronomy enable studying the properties of space-time and matter in superstrong gravitational fields. Images of the shadows of supermassive black holes in the sources M87 and Sgr A* obtained using the Event Horizon Telescope demonstrated the capabilities of ground-based VLBI [72, 73]. However, a more detailed study of the geometry of space-time and the properties of matter near the event horizon of supermassive black holes requires observations at shorter wavelengths and with larger interferometer bases. Therefore, the key task of the MSO in the ground-based interferometer mode will be to measure the geometry of space-time in the vicinity of the source Sgr A* in the center of the Galaxy and the vicinity of central supermassive black holes in the galaxies closest to us, including binary supermassive black holes, and to identify observational manifestations of wormholes [74–79].

Among the listed tasks, the search for wormholes (WHs), which are predicted by the General Theory of Relativity of objects [80–82], is of special importance for the development of basic science. The discovery of such objects will lead to a fundamental change in the scientific worldview and not only will prove the presence of a complex topology of space-time but also will make the existence of other universes real. In the early 2000s, N S Kardashev in collaboration with I D Novikov hypothesized that the nuclei of some galaxies may not be supermassive black holes but entrances to wormholes [83]. Due to the ultra-high angular resolution along with the high sensitivity of the MSO in the ground-space interferometer mode, this hypothesis can be tested using the characteristic observational differences between wormholes and black holes [78, 79, 84–86], such as the monopole magnetic field of a wormhole; differences between BHs and WHs in the shape and size of shadows and photon rings; the presence of a blue gravitational shift in the radiation from the outflow of matter from the WH entrance; and the possibility of observing radiation from the WH entrance.

Issues related to the emergence of life in the Solar System and in the Universe as a whole are of interest in terms of both general science and our world-view. The main task of the MSO project in this area is to study the origin and transport in

the Universe of water, one of the key components necessary for the origin of life on Earth.

It should be noted that, since the MSO research program is organized hierarchically based on key projects, which the main efforts (including observational time) will be directed toward implementing, next-level projects are also being developed, which are thematically related to the key ones. For example, second-level projects (presented in detail in [76]) include such urgent issues as the exploration of the Sunyaev–Zeldovich effect and relativistic corrections to it [87, 88]; observations of the first galaxies [89–91]; the detection and study of supermassive black holes (SMBHs) in the Universe at the turn of the reionization era [92] and their evolutionary features in 'dark' epochs $z \sim 10-30$ [93, 94]; examination of observational manifestations of the mutual influence of galaxies and massive black holes growing in their centers and identification of the mechanisms that determine their coordinated evolution; studying the evolution of galaxies in the 'midday' Universe (during the era of a global burst of star formation at $z \sim 2$) [95, 96] and the properties of infrared galaxies containing a large amount of dust [97]; and detection of gravitationally lensed systems to measure the Hubble constant H_0 [98, 99].

Regarding exploration of superstrong gravitational fields, it includes multi-frequency polarization observations of the immediate vicinity of black holes in SgrA* and M87* and the study of the nature of turbulence in the accretion flow based on these observations and estimating accretion flow parameters based on measurements of the multi-wavelength brightness distribution in the vicinity of SMBHs (~ 0.1 ms arc) in a wider SgrA* field, up to the Bondi radius of $\sim 0.03-0.1$ pc.

Studying the formation and transfer of water in the Universe includes the investigation of the filamentary structure of the interstellar medium, giant molecular clouds and star formation regions in the immediate vicinity of the Sun; examination of water transport into the inner regions of protoplanetary disks based on measurements of their spectral features; observational manifestations of the formation of terrestrial planets, the formation of habitable zones, the influence of variability and burst activity of central stars, red dwarfs, on the physical properties of disks within the supposed habitable zones; and the study of water reservoirs and measurement of its reserves in the Solar System.

5. Conclusion

The Spektr-R project, developed at the Astro Space Center LPI in collaboration with Russian industry, was not only an important stage in the development of radio astronomy in Russia but also the first successful major project of the Federal Space Program of the Russian Federation in many years. This project of the Federal Space Agency, the Russian Academy of Sciences, and the international scientific community, unparalleled in its scale and complexity, made it possible to obtain unique scientific results. During its implementation, the most important technologies for creating spacecraft for space research and corresponding service systems were developed. In addition, joint observations of the Spektr-R space radio telescope with a mirror diameter of 10 m and the largest ground-based radio telescopes yielded a ground-space radio interferometer with the longest base length, 350,000 km, which significantly improved the angular resolution of the observed objects compared to both ground-based radio interferometers and the previously implemented ground-space interferometer, VSOP.

The Millimetron Space Observatory (Spektr-M), a logical extension of the Spektr-R project into the shorter wavelength range of the electromagnetic spectrum using technologies of the next level of complexity, is also being developed at the Astro Space Center LPI. The creation of this observatory will be the next step in the development of space instrumentation technologies and large space structures, which will ultimately make it possible to implement the observatory's ambitious research program and solve a number of urgent problems in astrophysics.

In conclusion, we note that, along with the development of the Millimetron Space Observatory, the Astro Space Center LPI is promoting subterahertz astronomy in the Russian Federation. The concept of creating subterahertz instruments in the form of a universal compact antenna array to be deployed on the territory of the Russian Federation is being investigated [100]. Based on the concept of such an antenna array, it will also be possible to implement several space projects of a new generation in the subterahertz range — a space interferometer and a telescope located on the surface of the Moon. Ground-based antenna arrays will support the ground-space interferometer mode with the ultra-long base of the Millimetron observatory.

References

1. Kardashev N S et al. *Trudy Fiz. Inst. Ross. Akad. Nauk* **228** 112 (2000)
2. Kardashev N S et al. *Astron. Rep.* **57** 153 (2013); *Astron. Zh.* **90** (3) 179 (2013)
3. Sunyaev R et al. *Astron. Astrophys.* **656** A132 (2021)
4. Shustov B et al. *Astrophys. Space Sci.* **320** 187 (2009)
5. Smirnov A V et al. *Proc. SPIE* **8442** 84424C (2012)
6. Kardashev N S et al. *Phys. Usp.* **57** 1199 (2014); *Usp. Fiz. Nauk* **184** 1319 (2014)
7. Novikov I D et al. *Phys. Usp.* **64** 386 (2021); *Usp. Fiz. Nauk* **191** 404 (2021)
8. Predehl P et al. *Nature* **588** 227 (2020)
9. Pavlinsky M et al. *Astron. Astrophys.* **661** A38 (2022)
10. Hirabayashi H et al. *Science* **281** 1825 (1998)
11. Hirabayashi H et al. *Publ. Astron. Soc. Jpn.* **52** 955 (2000)
12. Thompson A R, Moran J M, Swenson G W (Jr.) *Interferometry and Synthesis in Radio Astronomy* (New York: Wiley, 2001); Translated into Russian: *Interferometriya i Sintez v Radioastronomii* (Moscow: Fizmatlit, 2003)
13. Matveenko L I, Kardashev N S, Sholomitskii G B *Sov. Radiophys.* **8** 461 (1965); *Izv. Vyssh. Uchebn. Zaved. Radiofiz.* **8** 651 (1965)
14. Kellermann K I et al. *Astrophys. J.* **153** L209 (1968)
15. Gubbay J et al. *Nature* **222** 730 (1969)
16. Kellermann K I et al. *Astrophys. J.* **169** 1 (1971)
17. Broderick J J et al. *Sov. Astron.* **14** 627 (1971); *Astron. Zh.* **47** 784 (1970)
18. Matveenko L I, Soobshch. IAA RAS No. 176 (St. Petersburg: Institute of Applied Astronomy RAS, 2007)
19. Kardashev N S, Pariiskii Yu N, Sokolov A G *Sov. Phys. Usp.* **14** 366 (1971); *Usp. Fiz. Nauk* **104** 328 (1971)
20. Zakson M B et al. *Zemlya Vselennaya* (4) 2 (1980)
21. Arsent'ev V M et al. *Sov. Phys. Dokl.* **27** 362 (1982); *Dokl. Akad. Nauk SSSR* **264** 588 (1982)
22. Levy G S et al. *Astrophys. J.* **336** 1098 (1989)
23. Linfield R P et al. *Astrophys. J.* **358** 350 (1990)
24. Aleksandrov Yu A et al. *Vestn. NPO im. S.A. Lavochkina* (3) 11 (2011)
25. Kardashev N S, Kovalev Y Y, Kellermann K I *Radio Sci. Bull.* (343) 22 (2012)
26. Shatskaya M V et al. *J. Astron. Instrum.* **11** 2250004 (2022)
27. Likhachev S F et al. *J. Astron. Instrum.* **6** 1750004 (2017)

28. Andrianov A S et al., in *Astronomical Data Analysis Software and Systems XXVI. Proc. of a Conf., 16–20 October 2016, Trieste, Italy* (ASP Conf. Ser., Vol. 521, Eds M. Molinaro, K Shortridge, F Pasian) (San Francisco, CA: Astronomical Society of the Pacific, 2019) p. 323
29. Likhachev S F et al. *Astron. Comput.* **33** 100426 (2020)
30. Kellermann K I, Pauliny-Toth I I K *Astrophys. J.* **155** L71 (1969)
31. Readhead A C S *Astrophys. J.* **426** 51 (1994)
32. Shklovskii I S *Sov. Astron.* **7** 748 (1964); *Astron. Zh.* **40** 972 (1963)
33. Lister M L et al. *Astron. J.* **152** 12 (2016)
34. Kovalev Y Y et al. *Adv. Space Res.* **65** 705 (2020)
35. Lister M L, in *Radio Astronomy at the Fringe, Green Bank, West Virginia, USA* (ASP Conf. Proc., Vol. 300, Eds J A Zensus, M H Cohen, E Ros) (San Francisco, CA: Astronomical Society of the Pacific, 2003) p. 71
36. Kardashev N S et al. *Vestn. NPO im. S.A. Lavochkina* (3) 4 (2016)
37. Kovalev Y Y et al. *Astrophys. J. Lett.* **820** L9 (2016)
38. Johnson M D et al. *Astrophys. J. Lett.* **820** L10 (2016)
39. Bruni G et al. *Astron. Astrophys.* **604** A111 (2017)
40. Gómez J L et al. *Astrophys. J.* **817** 96 (2016)
41. Giovannini G et al. *Nat. Astron.* **2** 472 (2018)
42. Lobanov A P et al. *Astron. Astrophys.* **583** A100 (2015)
43. Fuentes A et al. *Nat. Astron.* **7** 1359 (2023)
44. Savolainen T et al. *Astron. Astrophys.* **676** A114 (2023)
45. Kim J-Y et al. *Astrophys. J.* **952** 34 (2023)
46. Popov M V et al. *Astron. Rep.* **60** 792 (2016); *Astron. Zh.* **93** 778 (2016)
47. Popov M V et al. *Astrophys. J.* **888** 57 (2020)
48. Popov M V et al. *Mon. Not. R. Astron. Soc.* **465** 978 (2017)
49. Smirnova T V et al. *Astrophys. J.* **786** 115 (2014)
50. Shishov V I et al. *Mon. Not. R. Astron. Soc.* **468** 3709 (2017)
51. Andrianov A S et al. *Astron. Rep.* **61** 513 (2017); *Astron. Zh.* **94** 516 (2017)
52. Gwinn C R et al. *Astrophys. J.* **822** 96 (2016)
53. Fadeev E N et al. *Mon. Not. R. Astron. Soc.* **480** 4199 (2018)
54. Baan W A et al. *Nat. Astron.* **6** 976 (2022)
55. Bayandina O S et al. *Adv. Space Res.* **65** 763 (2020)
56. Sobolev A M et al. *Astrophys. J.* **856** 60 (2018)
57. Litvinov D A et al. *Phys. Lett. A* **382** 2192 (2018)
58. Nunes N V et al. *Adv. Space Res.* **65** 790 (2020)
59. Nunes N V et al. *Class. Quantum Grav.* **40** 175005 (2023)
60. Rudnitskiy A G et al. *Acta Astronaut.* **196** 29 (2022)
61. Golubev E S et al. *Proc. SPIE* **11451** 114510K (2020)
62. Arkhipov M et al. *J. Astron. Telescop. Instrum. Syst.* **7** 044001 (2021) https://doi.org/10.1117/1.JATIS.7.4.044001
63. Khudchenko A et al. *Proc. SPIE* **12190** 121902W (2022)
64. Khudchenko A et al. *IEEE Trans. Terahertz Sci. Technol.* **13** 645 (2023)
65. Tretyakov I V, Khudchenko A V, Chernii R A, Likhachev S F *J. Commun. Technol. Electron.* **68** 989 (2023); *Radiotekh. Elektron.* **68** 904 (2023)
66. Likhachev S F et al. *Mon. Not. R. Astron. Soc.* **511** 668 (2022)
67. Zeldovich Ya B, Sunyaev R A *Astrophys. Space. Sci.* **4** 301 (1969)
68. Sunyaev R A, Zeldovich Ya B *Astrophys. Space Sci.* **7** 20 (1970)
69. Novikov D I, Mihalchenko A O *Phys. Rev. D* **107** 063506 (2023)
70. Maillard J-P et al. *Phys. Rev. D* **109** 023523 (2024)
71. Silk J *Astrophys. J.* **151** 459 (1968)
72. Event Horizon Telescope Collab., Akiyama K et al. *Astrophys. J. Lett.* **875** L1 (2019)
73. Event Horizon Telescope Collab., Akiyama K et al. *Astrophys. J. Lett.* **930** L12 (2022)
74. Andrianov A S et al. *Mon. Not. R. Astron. Soc.* **500** 4866 (2021)
75. Chernov S V *J. Exp. Theor. Phys.* **132** 897 (2021); *Zh. Eksp. Teor. Fiz.* **159** 1018 (2021)
76. Novikov I D, Repin S V *Astron. Rep.* **65** 3 (2021); *Astron. Zh.* **98** 3 (2021)
77. Andrianov A et al. *Phys. Rev. D* **105** 063015 (2022)
78. Bugaev M A et al. *Phys. Rev. D* **108** 124059 (2023)
79. Chernov S V *Astron. Rep.* **67** 798 (2023); *Astron. Zh.* **100** 693 (2023)
80. Flamm L, Schumann R *Phys. Z.* **17** 448 (1916)
81. Einstein A, Rosen N *Phys. Rev.* **48** 73 (1935)
82. Wheeler J A *Phys. Rev.* **97** 511 (1955)
83. Kardashev N S, Novikov I D, Shatskiy A A *Int. J. Mod. Phys. D* **16** 909 (2007)
84. Tsukamoto N, Harada T, Yajima K *Phys. Rev. D* **86** 104062 (2012)
85. Novikov I D *Phys. Usp.* **61** 280 (2018); *Usp. Fiz. Nauk* **188** 301 (2018)
86. Ishkaeva V A, Sushkov S V *Phys. Rev. D* **108** 084054 (2023)
87. Sunyaev R A, Zeldovich Ya B *Astrophys. Space. Sci.* **9** 368 (1970)
88. Novikov D I et al. *Phys. Rev. D* **101** 123510 (2020)
89. Larchenkova T I et al. *Astrophysics* **65** 161 (2022); *Astrofizika* **65** 179 (2022)
90. Nath B B et al. *Mon. Not. R. Astron. Soc.* **521** 662 (2023)
91. Pilipenko S V, Ermash A A, Bendo G *Astron. Rep.* **66** 296 (2022); *Astron. Zh.* **99** 297 (2002)
92. Ferrara A, in *Understanding the Epoch of Cosmic Reionization: Challenges and Progress* (Astrophysics and Space Science Library, Vol. 423, Ed. A Mesinger) (Cham: Springer, 2016) p. 163, https://doi.org/10.1007/978-3-319-21957-8_6
93. Vasiliev E O, Shchekinov Yu A, Nath B B *Astrophysics* **65** 324 (2022); *Astrofizika* **65** 333 (2022)
94. Vasiliev E O, Shchekinov Yu A *Astrophys. J.* **887** 174 (2019)
95. Spinoglio L et al. *Publ. Astron. Soc. Aust.* **34** 57 (2017)
96. Spinoglio L et al. *Publ. Astron. Soc. Aust.* **38** 21 (2021)
97. Casey C M, Narayanan D, Cooray A *Phys. Rep.* **541** 45 (2014)
98. Larchenkova T I, Ermash A A, Doroshkevich A G *Astron. Lett.* **45** 821 (2019); *Pis'ma Astron. Zh.* **45** 866 (2019)
99. Larchenkova T I, Lyskova N S, Lutovinov A A *Astron. Lett.* **37** 441 (2011); *Pis'ma Astron. Zh.* **37** 483 (2011)
100. Likhachev S F et al. *Cosmic Res.* **62** 117 (2024); *Kosm. Issled.* **62** 121 (2024)